On Pellet-Induced Charge Exchange Effects in Ohmically Heated and NB Heated Tokamak Plasmas

L.Lengyel

IPP 1/213

March 1983

MAX-PLANCK-INSTITUT FÜR PLASMAPHYSIK

8046 GARCHING BEI MÜNCHEN

MAX-PLANCK-INSTITUT FÜR PLASMAPHYSIK

GARCHING BEI MÜNCHEN

On Pellet-Induced Charge Exchange Effects in Ohmically Heated and NB Heated Tokamak Plasmas

L.Lengyel

IPP 1/213 March 1983

Die nachstehende Arbeit wurde im Rahmen des Vertrages zwischen dem Max-Planck-Institut für Plasmaphysik und der Europäischen Atomgemeinschaft über die Zusammenarbeit auf dem Gebiete der Plasmaphysik durchgeführt.

On Pellet-Induced Charge Exchange Effects in Ohmically Heated and NB Heated Tokamak Plasmas

L.Lengyel
Max-Planck-Institut für Plasmaphysik, EURATOM Association,
D-8046 Garching, Germany

This report describes in detail the paper 9W5, presented at the 24th Annual Meeting of the Amer. Phys. Soc. in New Orleans, Louis., Nov. 1982.

Introduction

The purpose, advantages, and disadvantages of pellet injection in tokamak plasmas have been extensively discussed in the literature (see, for example /1,2/). Pellet injection has become a frequently used method of replacing particle losses in divertor tokamaks /3,4,5/ and of depositing particles at depths not accessible to gas puffing /6,7/. Pellets can also be used as markers for diagnostic puroses, or for building-up high-density target plasmas for neutral beam injection /6,8/.

In early analyses pertaining to the effect of pellets on the recipient plasmas it was always assumed that the pellet particles are almost instantaneously ionized at the ablation site /9/ and interact as ions with the background plasma and the confining magnetic field. Calculations in which pellets as possible local neutral particle sources were considered /10,11/ have shown some notable differences, both qualitatively and qantiatively, compared with the ion source approximation. It was suggested in /11/ that charge exchange collisions may be responsible for the differences noted. Measurements on ASDEX and PDX (see, for example, /5/) showed plasma parameter changes at some distance from the pellet ablation region with a time delay so short that it could not be explained on the basis of the known classical and anomalous transport processes. (The possibility of instantaneous plasma mixing due to sawtooth-like oscillations in regions outside the pellet deposition zone is not considered here.)

It was thus decided to perform calculations for experimental plasma conditions by applying a transport code that incorporates Monte Carlo simulation of the neutral particle transport (1D PPPL transport code BALDUR /12/). The primary objectives of these calculations were to obtain information on the effect of cx coolisions on the pellet particle depositon profile and the plasma parameter distributions, and to obtain information on the magnitutes of the resulting particle and energy losses both in ohmically and NB-injection-heated plasmas.

Computational Model

A detailed description of the transport code can be found in /12/. The modified version of the code used here allowed for the existence of a 10 cm wide scrape-off layer outside the separatrix. The code was supplemented by an ablation routine based on the neutral gas shielding model of Milora and Foster /13/. In some calculations, ablation due solely to NB-produced fast ions was considered. In all runs it was assumed that the ablation takes place on a time scale much shorter (a factor of 10^{-2} to 10^{-3}) than any of the relevant transport processes taking place in the plasma - an assumption that may not necessarily be true if transport by cx collisions is taken into account. As a result of this assumption, the pellet ablation and pellet particle deposition profile could be computed under "frozen-in" plasma parameter conditions by only taking into account the instantaneous adiabatic cooling (and density step-up) of the plasma in each differential flux tube by the deposited pellet particles. (A particularly of the BALDUR code: the adiabatic mixing of pellet particles with the plasma is only taken into account in the ablation rate calculations. The transport calculations are renewed by starting with the original "frozen-in" plasma parameter values.)

Two options are offered at this point: the ablated pellet particles (all or some of them) can either be treated as ions and added to the corresponding ion source terms, or assumed to be neutral particles, transferred and added to the neutral volume source terms and then processed by a 1D Monte Carlo routine available in BALDUR.

The standard input data set of BALDUR was supplemented by three new parameters: (a) the bulk ionization degree of the pellet η,

i.e. the fraction of the ablated particles that is treated as an ion source term. Since neither the local ion temperature in the ablation cloud nor the temperature distributions in its neighbourhood are known, it is rather difficult to estimate, on the basis of the existing theoretical models, the relative weights of cx and ionizing collisions (i.e. the effective value of η) in the region of strong pellet-plasma interaction. Therefore, for assessing the quantitative effects of cx collisions, only the limiting cases $\eta = 1$ and $\eta = 0$ are considered and compared in the present calculations. These two cases correspond to a "fully ionized" pellet, and to a pellet that interacts as neutral gas with the recipient plasma. (b) The temperature of the neutral particles added to the respective source term was assumed to be 10^{-3} eV. (The exact value of this temperature does not play any significant role as long as it is substantially lower than the local ion temperature. Temperature values up to 10 eV were tested.) (c). To define a local neutral particle source, one needs the rate of neutral deposition at each mesh point. In the present approximation we calculate the pellet ablation (i.e. particle deposition) profile corresponding to a global (total) pellet lifetime. This may be a good approximation for the $\eta = 1$ case, but not necessarily for the neutral pellet approximation (here cx collisions may redistribute the sources during the pellet flight-time). Nevertheless, in the present calculations the local neutral source strength was defined with the help of the pellet lifetime: the number of neutral particles deposited at a mesh point has been divided by the product of the pellet lifetime τ_{pel} and a scaling factor C_{ns}, whereas C_{ns} was an input parameter. All results reported here corresponds to $C_{ns} = 1$.

An NB-heated ASDEX discharge of approximately 1.8 s duration was used as reference (i.e. recipient) discharge. The discharge was ohmically heated during the build-up phase and by NB injection from t = 1.42 s to t = 1.62 s. The temporal characteristics of the discharge without pellet were simulated with a suitable se-

lection and combination of the transport processes available in BALDUR. The ion heat conduction was assumed to be neoclassical and the anomalous particle and electron thermal transport were described by the empirical expressions:

$$\chi_e = 1.9 \times 10^{17}/n_e T_e \quad \text{for } r < r_{scr},$$
$$D = 0.2\,\chi_e \quad \text{for } r < r_{scr},$$
$$\chi_e = 3.2 \times 10^{4} \quad \text{for } r > r_{scr},$$
$$D = 1.6 \times 10^{3} \quad \text{for } r > r_{scr}.$$

Bohm-like diffusion was assumed for the region inside the q = 1 surface. A recycling coefficient 0.2 was assumed (divertor regime). The same transport scaling was used for the NB injection phase as for the ohmic heating phase. Therefore the temperatures calculated for the NB phase are higher than the measured experimental values /14/.

In this reference plasma a pellet was injected at a certain time: t_{pel} = 1.00 s (ohmic discharge phase), or t_{pel} = 1.50 s (NB-heating phase), or t_{pel} = 1.625 s (post-NB discharge phase). The pellet size corresponds to an average plasma density of 6.2×10^{12} cm^{-3} in the discharge volume considered (scrape-off layer included).

The basic discharge data, the NB-injection and pellet parameters used in the simulation runs are given in Table I. The plasma parameters prevailing prior to pellet injection are summarized in Table II for the three cases considered. In the same Table, the total pellet penetration depths (scrape-off layer thickness and a fraction of the plasma radius) corresponding to different pellet velocities as well as the maximum T_e and n_e values "seen" by the ablating pellets are also shown.

Results of Calculations

Ohmic heating phase: t_{pel} = 1.00 s

Single pellets were injected in the ASDEX plasma with two different velocities: 250 m/s and 750 m/s (see Figs. 1 to 4). At the lower velocity, the ablation ended at r = 50 - ℓ_{pel} = 19 cm. At the higher velocity, the pellet has almost reached the plasma centre (r = 50 - 45 = 5 cm). Figures 1 and 2 show the time variation

of the central and volume-averaged electron densities n_{eo} and $\langle n_e \rangle$, respectively, for a "fully ionized" pellet ($\eta = 1$) and for a pellet that interacts as neutral gas with the recipient plasma. There are some notable differences in the plasma parameter variations corresponding to the two cases.

In the low-velocity case, if $\eta = 1$ is assumed, there is a time delay observable between the completion of the pellet ablation and the density rise in the plasma center. This time delay is the diffusion time. If $\eta = o$ is assumed, an almost instantaneous density rise is observed at the plasma center upon pellet injection. Further-on, the density rise follows the diffusion pattern. The instantaneous density change is due to cx collisons: cx neutrals transverse the plasma with thermal velocities corresponding to the ion temperature at the site of their birth and become ionized at some distance from the pellet location, thus contributing to the local ion (and electron) density. In the low pellet velocity case, cx collisions yield a higher peak central density value than the pure diffusion resulting from the $\eta = 1$ assumption. At the higher velocity, the pellet is injected almost up to the plasma center. Accordingly, there is no difference between the rise times due to cx and diffusion,and cx collisions can only contribute to the removal of particles from the central region. As a result of this, here the central density peak obtained with $\eta = o$ lies below the value corresponding to $\eta = 1$ (see Fig. 2). (The absolute values of the differences between the curves $\eta = o$ and $\eta = 1$ in Figs. 1 and 2 are rather small; they merely indicate tendencies.) Note that the absolute value of the central density peak is considerably higher at deep penetration, and the particle confinement time is longer (approximately 27 ms compared with 9 ms) then at smaller pellet penetration. The assumptions $\eta = o$ and $\eta = 1$ do not seem to produce substantial differences in the time variation of n_e either at low or at high velocities (negligible particle losses).

The volume-averaged value of the cx losses during pellet injection is shown for the two pellet velocities used in Fig. 3 ($\eta = o$). The peak values shown correspond to 15-fold and 70-fold increases of

the cx losses, respectively. Measurements performed on PDX /16/ under comparable plasma conditions (ohmically heated plasma, T_{eo} = 500 to 600 eV, v_{pel} = 500 m/s) showed in fact a strong enhancement of the cx signals. The variation of the energy content of the plasma is shown in Fig. 4 for the two cases considered here. As can be seen, with η = o an instantaneous decrease of the plasma energy occurs upon pellet injection, which is caused by the energetic cx neutrals leaving the plasma. The energy loss is higher at deeper pellet penetration: the cx neutrals originate from hotter plasma regions (for the given plasma conditions the magnitude of the cx losses is still rather small: it is about 6 % at v_p=750 m/s).

NB injection phase: t_{pel} = 1.500 s

Results relating to pellet injection during NB heating are shown in Figs. 5 to 14. The first four of these correspond to a pellet velocity of 250 m/s.

The time variations of the central electron and ion densities following pellet injection are shown in Figs. 5 and 6, respectively. The difference between the η = o and η = 1 cases is obvious: practically instantaneous density increase in the plasma centre due to cx transport in the η = o case, and delayed increase owing to longer diffusion times in the η = 1 case. The central electron density variation displays another interesting characteristic, both in the η = o and the η = 1 cases: it first decreases (for about 10 to 20 ms) from its initial value (cx peak if η = o) and increases again when diffusing particles reach the center. This inital decrease is due to the interception of the neutral beam particles by the enhanced plasma density in the outer layers. While the density of the thermal ions is still being built up by means of classical slow-down of the fast (NB) ions still present in the plasma center, the rate of the electron density is directly coupled to the NB source. Sudden changes in the NB particle flux instantaneously affect the local electron density.(The difference between the numerical values in Figs. 5 and 6 is due to the accounting procedure in BALDUR. Fig. 6 represents the central density of the thermal

ions, whereas the electron density includes two components: the electrons of the recipient (thermal) plasma and those of the fast (non-thermal) NB ions that have not yet been slowed down.)

The time variations of the central and volume-averaged electron and ion temperatures are shown in Figs. 7 and 8, respectively. With η = o, the central temperatures show an immediate, although weak, response (approximately 6 % and 2 % for the electrons and ions) and the usual diffusion caused delayed response if η = 1 is assumed. More pronounced is the effect on the average temperatures, particularly in the case of the ion component. The difference between the η = 1 and the reference (i.e. no pellet) curves is due to the adiabatic cooling of the plasma by the pellet, whereas the difference between the η = o and η = 1 curves is a pure cx loss effect and is not recoverable.

Figure 9 represents the variation of n_e(r = o) corresponding to a slightly higher pellet velocity. As a result of deeper penetration and less effective shielding of the center from NB particles, the dip in the n_{eo} curves is reduced. Going to still higher pellet velocities eliminates this shielding effect altogether (see Figure 10).

Figures 10 to 14 correspond to a pellet velocity of v_{pel} = 700 m/s. The immediate density and temperature responses at the plasma center triggered by cx collisions have become more pronounced (approximately 12 % density change) and the dip in the electron density variation has disappeared (see Fig. 10 and 11). The central ion temperature change is about 13 %, and the jump in the electron temperature is about half as large (Fig. 12). The change of the volume-averaged value of the ion temperature is quite pronounced: it is 59 % with η = o and 37 % with η = 1, i.e. 37 % of the total temperature drop is due to cx losses (see Fig. 13).

Figure 14 shows the increase of the cx losses during pellet injec-

tion. Owing to the higher ion temperatures inherent in the NB injection phase, these losses are considerably higher than during the ohmic heating phase (cf. Fig. 3). The corresponding increase of the Fe sputtering rate, as calculated by BALDUR, would be 140-fold, 84-fold and 59-fold, corresponding to the pellet velocities 700, 400 and 250 m/s, respectively. However, owing to the relatively short duration of the ablation process, the total number of sputtered particles is relatively low.

Post-NB discharge phase: t_{pel} = 1.625 s

In a series of calculations, pellets were injected into the discharge 5 ms after the NB injection cut-off but still within the fast ion slow-down time. As can be seen from Table 2, this case differs from the previous ones in that the central and average temperatures are much higher. The pellet particles thus interact here with a hotter plasma, and so the cx effects are expected to be more pronounced. The results of these simulation runs are shown in Figs. 15 to 19.

The changes of the central densities and temperatures of the electrons and ions are shown in Figs. 15 and 16, respectively. Owing to the poor penetration of the pellet into the plasma, the quantitative change of these parameters is not significant (T_{io}: 10 %, T_{eo} = 5 %, n_{eo} and n_{io}: 5 %). The changes of their volume-averaged values are shown in Figs. 17 and 18. A substantial effect can be observed on the average temperature curves: the average ion temperature drops by 58 %. About 33 % of this temperature drop is solely due to cx losses. This can readily be seen from Fig. 19, where the plasma energy is plotted. While with η = 1 the energy content even increases over the reference value (no pellet) because of the more rapid thermalization of the fast ions in a dense plasma, the energy content drops by approximately 20 % if the pellet particles interact as neutrals with the background plasma.

Beam thermalization

The effect of a pellet on the thermalization of NB particles is summarized in Table 3. All quantities displayed have been reduced

by means of the respective reference (no pellet) quanities. As can be seen, if the pellet particles are assumed to interact as ions with the beam plasma ($\eta = 1$), i.e. if the background density is instantaneously stepped-up, the higher energy groups of the fast ions become depleted and the lower ones get filled up above their reference values. The cx losses of the beam ions are effectively reduced (30 to 40 %, depending upon the penetration depth) and the plasma heating rate increases by a factor of almost 2. If the pellet particles interact as neutrals with the rest of the particles ($\eta = o$), all energy groups become severely depleted (the lower the fast ion energy the larger is the population depletion) and a substantial number of particles are scattered out of the plasma (20 to 40 %,depending upon the pellet penetration depth). The energy losses of the beam due to cx collisions increase by a factor of 30 to 50 during the ablation, depending upon the pellet velocities considered. The plasma heating rate is reduced to between 84 and 67 % of the respective reference values. Hence, according to the BALDUR-results, it may not necessarily be advantageous to increase the plasma density by pellet injection during the NB injection phase.

Ablation due to fast (NB) ions

In a series of simulation runs, the neutral shiedling ablation model of Milora and Foster was replaced by a model in which ablation was assumed to be solely due to stopping the NB ions of the different energy groups in the ablation cloud. The ion-energy-dependent stopping cross-sections were taken from /17/ and incorporated in the semi-empirical shielding expression of Milora and Foster. Figures 20 and 21 show the radial electron density distributions immediately after pellet injection for the $\eta = o$ and $\eta = 1$ cases. The practically instantaneous smear-out effect of the cx collisions is apparent and is the same irrespective of whether the ablation is caused by thermal electrons, fast ions, or any other plasma constituents. The decisive factor in this respect is the ionization state of the pellet particles interacting with the beam and the plasma.

Since it is rather uncertain how neutral gas shielding functions when various plasma species (thermal particles, fast ions, runaway electrons, etc.) simultaneously interact with the pellet, no extensive calculations were perfomed with this NB ion ablation model. To have any degree of confidence in computational results of this kind, one would need a better founded ablation model that takes into account the ablation dynamics and the build-up of a shielding layer under the simultaneous action of different energy carriers.

Conclusions

The results of these simulation calculations show, for the assumptions outlined at the beginning of this report and within the accuracy limits of the BALDUR code, that if the pellet particles interact as neutrals with the recipient plasma, the effects caused by cx collisions may be quite substantial, depending upon the discharge regime and pellet parameters. The more important of these effects are as follows:

(1) Charge exchange collisions may induce measurable plasma parameter changes at locations far from the pellet deposition site on a time scale much shorter than τ_{diff}.

(2) Plasma particle losses caused by pellet-induced cx collisions are, in general, negligible. This is not necessarily true for fast (NB) ions if pellet injection is combined with NB injection.

(3) Energy losses due to cx collisions may be significant both for the background plasma and for the NB. It is primarily the ions that are affected, the temperature change of the electron being only a fraction of that of the ions.

(4) The pellet velocities required for deep pellet penetration (central refuelling) may be relaxed if neutral transport due to cx collisions is taken into account, but:

(5) The selection of optimum pellet velocity-mass-frequency combinations should in any case be based on detailed transport calculations. The results may be quite different for different discharge regime and pellet parameter combinations.

(6) The characteristics of NB heating may be significantly changed if the pellet is injected during the heating phase.

(7) The question what fraction of the pellet particles interact as neutrals with the plasma is still open. The answer to this question requires a better understanding of the details of the pellet ablation and ionization dynamics, particularly in the presence of different kinds of energy carriers.

References

/1/ S.L.Milora, J.Fusion Energy 1 (1981), 15 - 48

/2/ L.L.Lengyel, Phys. Fluids 21 (1978), 1945 - 1956

/3/ K.Büchl, G.C.Vlases, Bull. Amer. Phys. Soc. 24 (1981), p. 888; G.C.Vlases and L.L.Lengyel, Bull. Amer. Phys. Soc. 27 (1982), 8, p. 1128

/4/ G.L.Schmidt et al., Bull. Amer. Phys. Soc. 27 (1982), 8, p. 1049

/5/ D.J.Campbell and A. Eberhagen, to be published; see also S.L.Milora et al., Nucl. Fusion 22 (1982), 1263 - 1271

/6/ S.L.Milora et al., Nucl. Fusion 20 (1980), 1491 - 1514

/7/ C.M.Greenwald et al., Bull. Amer. Phys. Soc. 27 (1982), 8, p. 1037

/8/ H.Ringler, Bull. Amer. Phys. Soc. 27 (1982), 8, p. 1068

/9/ A.T.Mense et al., ORNL Rept. TM-6026, (1978)

/10/ L.L.Lengyel and D.F.Düchs, Proc. 10th SOFT, Padova (1978) 283 - 288

/11/ L.L.Lengyel, Zeitschrift f. Naturforschung 34a (1979), 957 - 963 (in English)

/12/ D.E.Post et al., TFTR Physics Group, PPPL Rept. No. 33 (1981)

/13/ S.L.Milora and C.A.Foster, IEEE Transact. Pl. Sci. PS-6 (1978), 578 - 592

/14/ G.Becker at al., Nucl. Fus. 22 (1982), 1589 - 1595

/15/ J.A.Phillips, Phys. Rev. 90 (1953), 532

Table 1: ASDEX, neutral beam, and pellet data used in numerical simulation (hydrogen-deuterium target plasma, hydrogen neutral beams, hydrogen pellets).

ASDEX	NB	Pellet
$R = 165$ cm	$E_{NB} = 40$ keV	$N_p = 4.82 \times 10^{19}$
$a = 40$ cm	$E_{1/1} = 0.333$	$r_p = 0.06$ cm
$l_{scr} = 10$ cm	$E_{1/2} = 0.333$	$v_p = 250$ m/s
$B = 22$ kG	$E_{1/3} = 0.333$	to
$I = 320$ kA	$I_{NB} = 98$ A	750 m/s
$N_{total} = 8.3 \times 10^{19}$ to 1.48×10^{20}	$t_{on} = 1.42$ s	$t_p = 1.00$ s
	$t_{off} = 1.62$ s	1.50 s
		1.63 s

Table 2: Discharge parameters before pellet injection and penetration data

Parameter	t = 1.00 s		t = 1.500 s		t = 1.625 s
$\langle n_e \rangle$ cm^{-3}	1.90×10^{13}		1.18×10^{13}		1.06×10^{13}
$\langle T_e \rangle$ keV	0.215		1.280		2.130
$\langle T_i \rangle$ keV	0.200		2.270		4.830
n_{eo} cm^{-3}	2.99×10^{13}		4.42×10^{13}		4.30×10^{13}
T_{eo} keV	0.70		1.80		2.98
T_{io} keV	0.50		3.17		6.37
	Pellet penetration data				
pellet velocity $(\frac{m}{s})$	250	750	250	700	750
l_{pel} cm	31	45	25	32	29
$T_e\ (l)_{max}$ keV	0.386	0.689	0.988	1.610	2.20
$n_e\ (l)_{max}$ cm^{-3} (10^{13})	2.87	2.98	1.86	3.25	2.38

Table 3: Effect of pellet on beam thermalization and plasma heating. t_{pel} = 1.500 s
(all values represent, unless otherwise indicated, percentages of the respective reference, i.e. "no pellet case", values)

Deplation of beam energy groups: Energy level (kev)	v_{pel} = 250 m/s		v_{pel} = 700 m/s	
	$\eta = 1$	$\eta = 0$	$\eta = 1$	$\eta = 0$
4	146	54	154	35
8	103	75	102	56
12	96	79	97	59
16	96	80	96	60
20	91	82	91	63
24	101	82	104	63
28	99	82	102	63
32	95	83	99	64
36	91	83	82	64
40	83	86	79	70
Total number of beam particles present	97	79	98	60
CX-losses of the beam	62	30-fold	72	54-fold

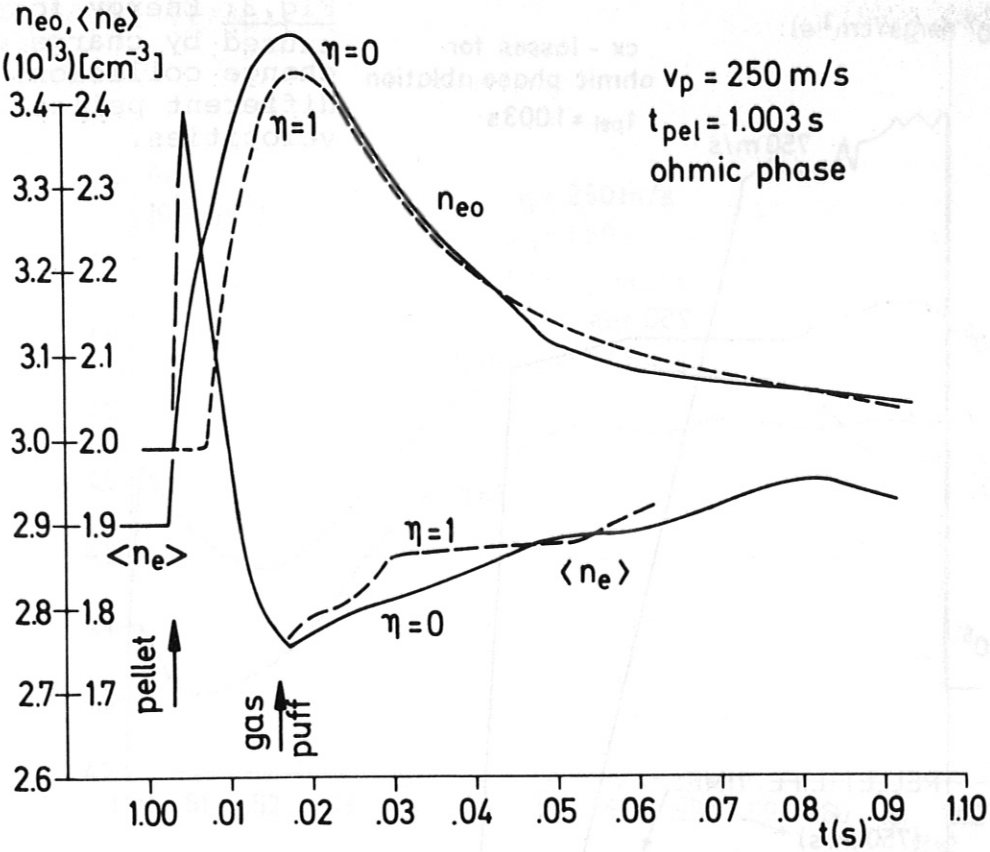

Fig. 1: Time variation of the central and average electron densities following pellet injection.

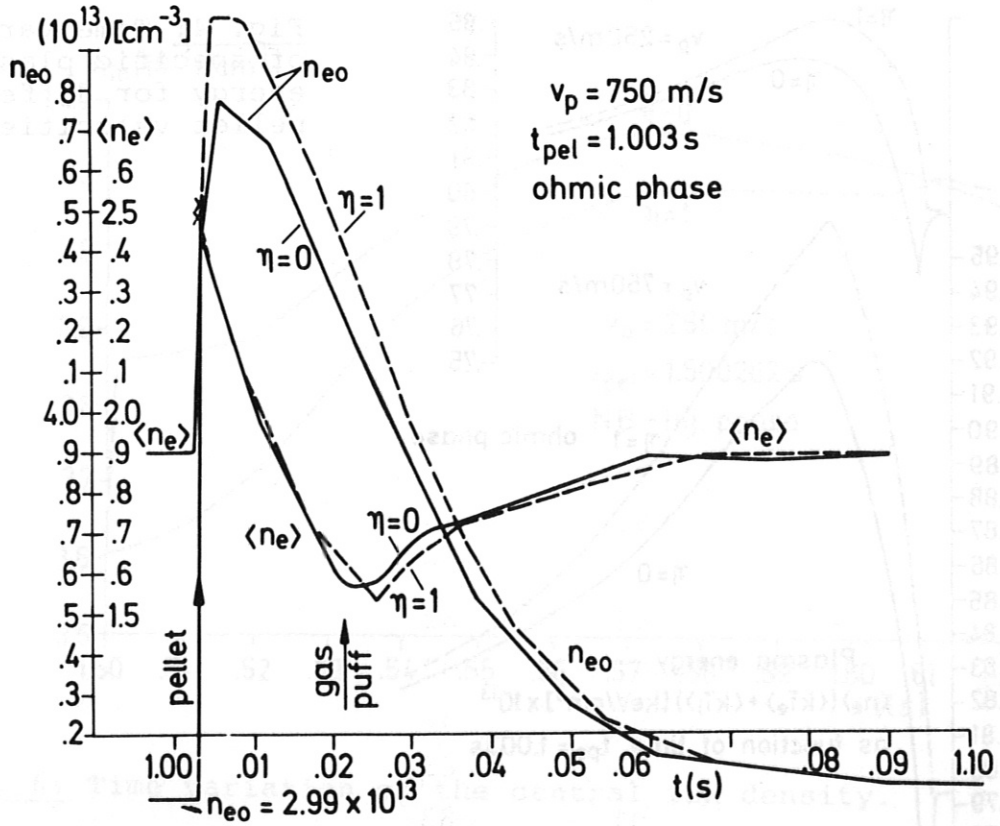

Fig. 2: Time variation of the central and average electron densities following pellet injection.

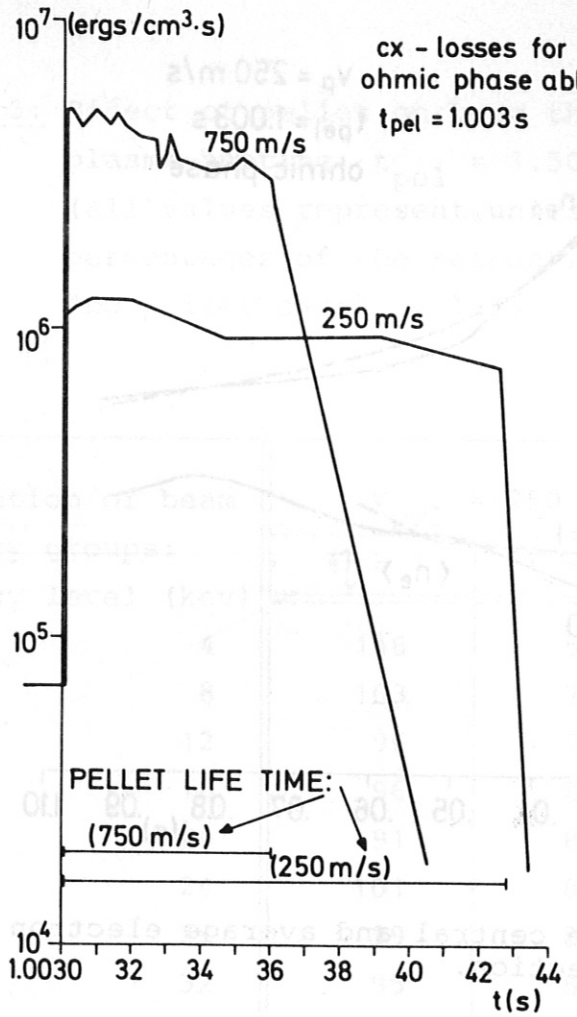

Fig.3: Energy losses caused by charge exchange collisions for different pellet velocities.

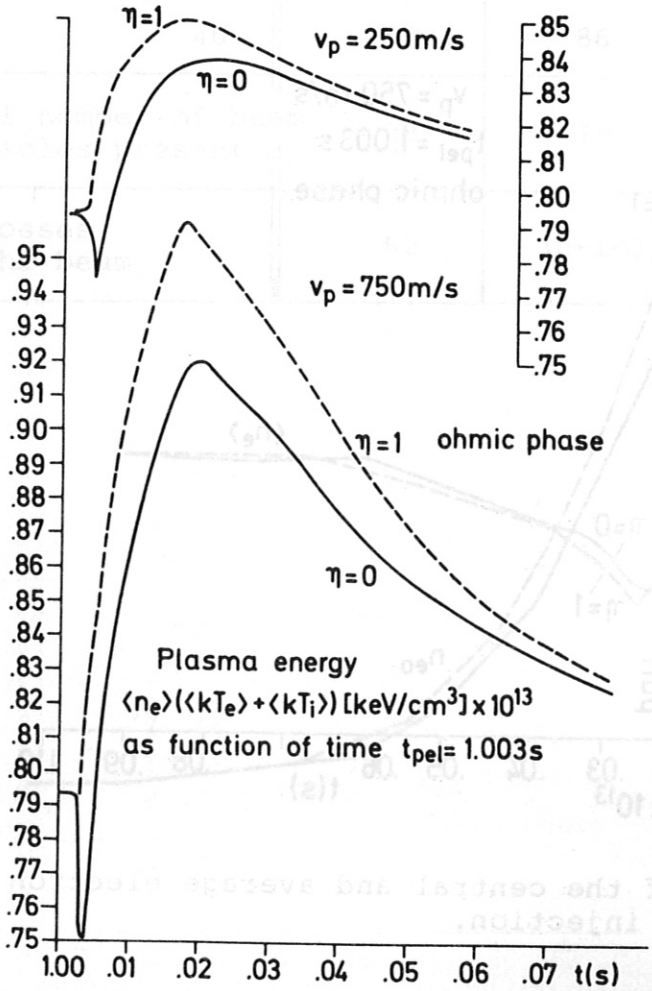

Fig. 4: Time variation of specific plasma energy for different pellet velocities.

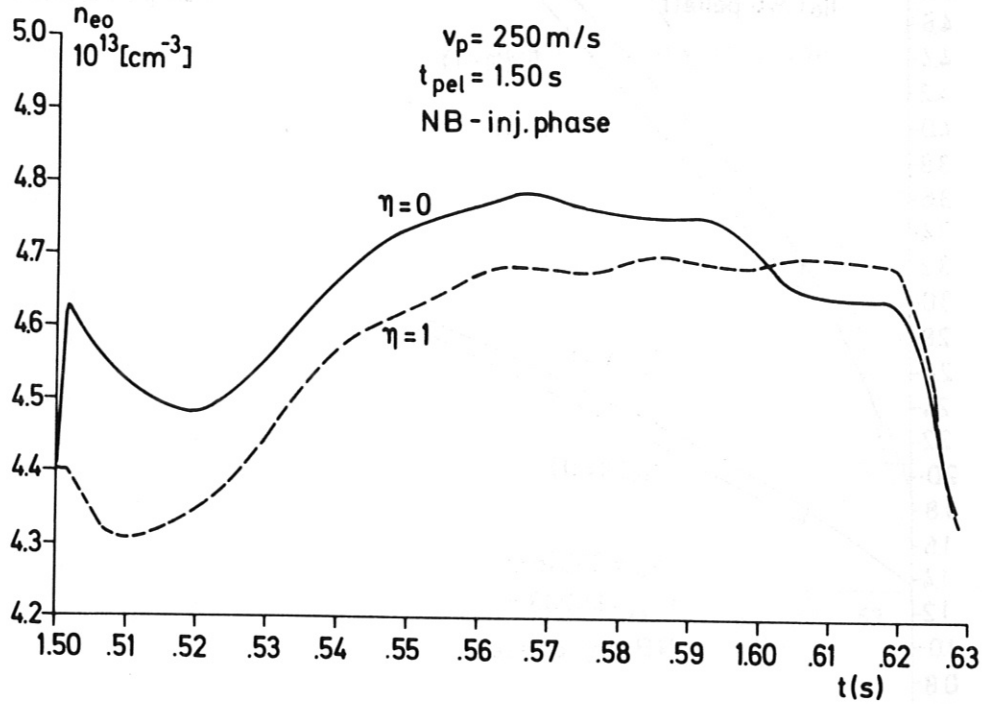

Fig. 5: Time variation of the central electron density.

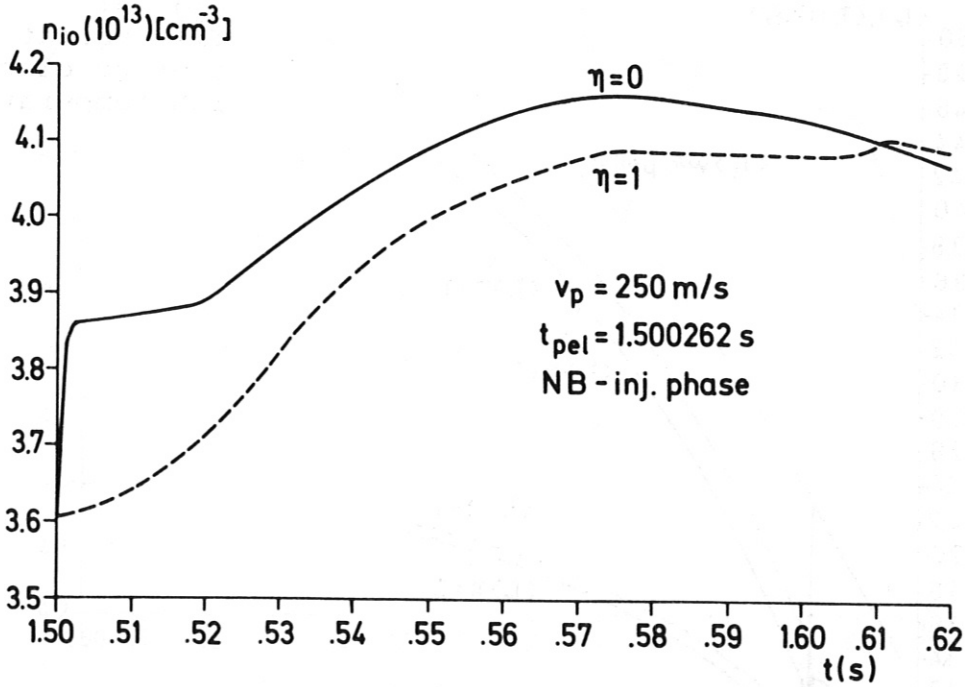

Fig. 6: Time variation of the central ion density.

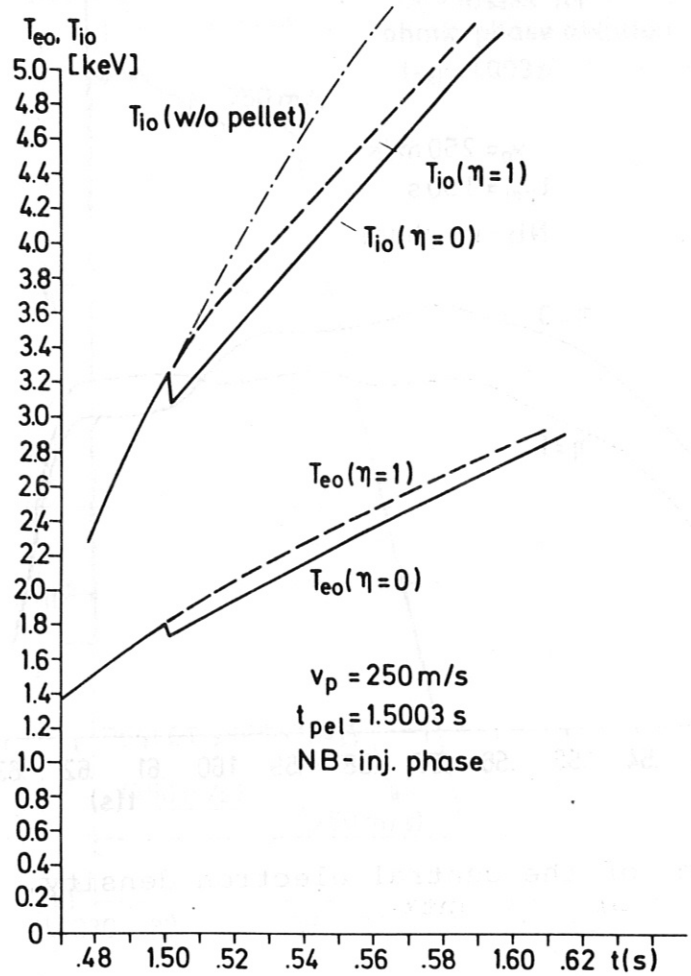

Fig. 7:
Time variation of central electron and ion temperatures.

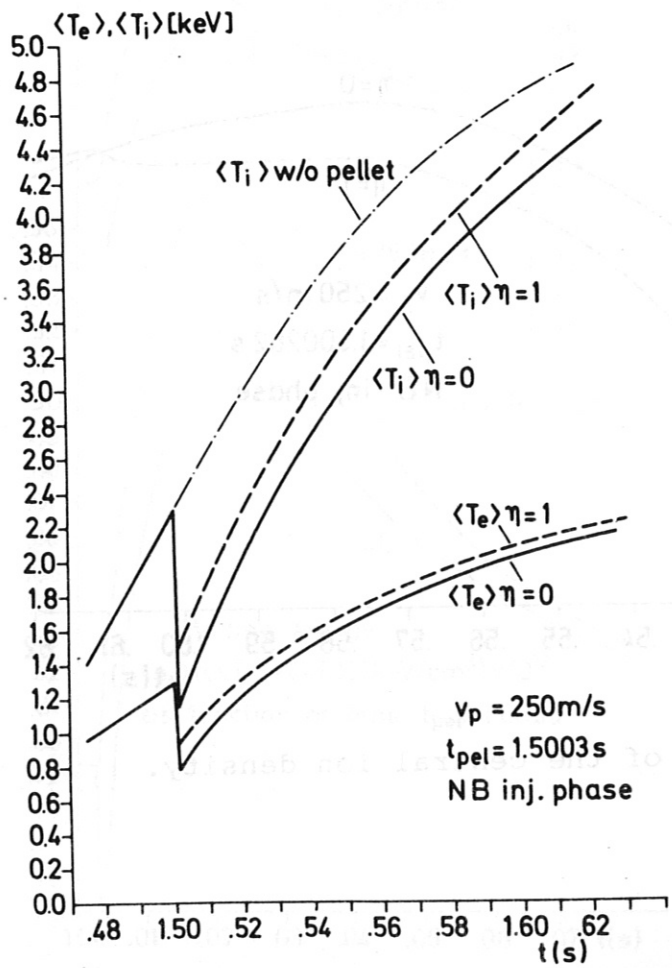

Fig. 8:
Time variation of average electron and ion temperatures.

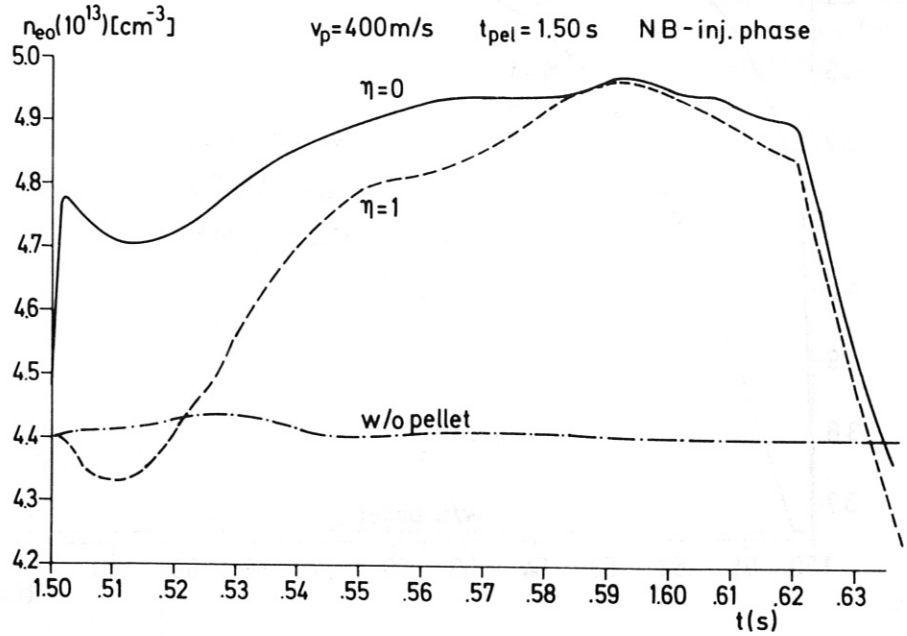

Fig. 9: Time variation of the central electron density for an intermediate pellet velocity.

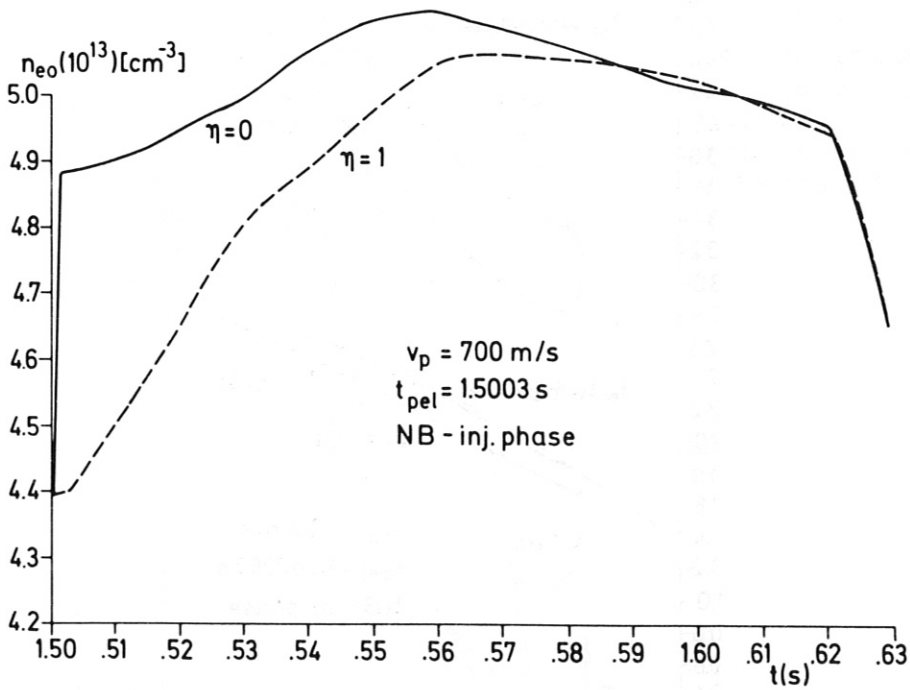

Fig. 10: Time variation of the central electron density.

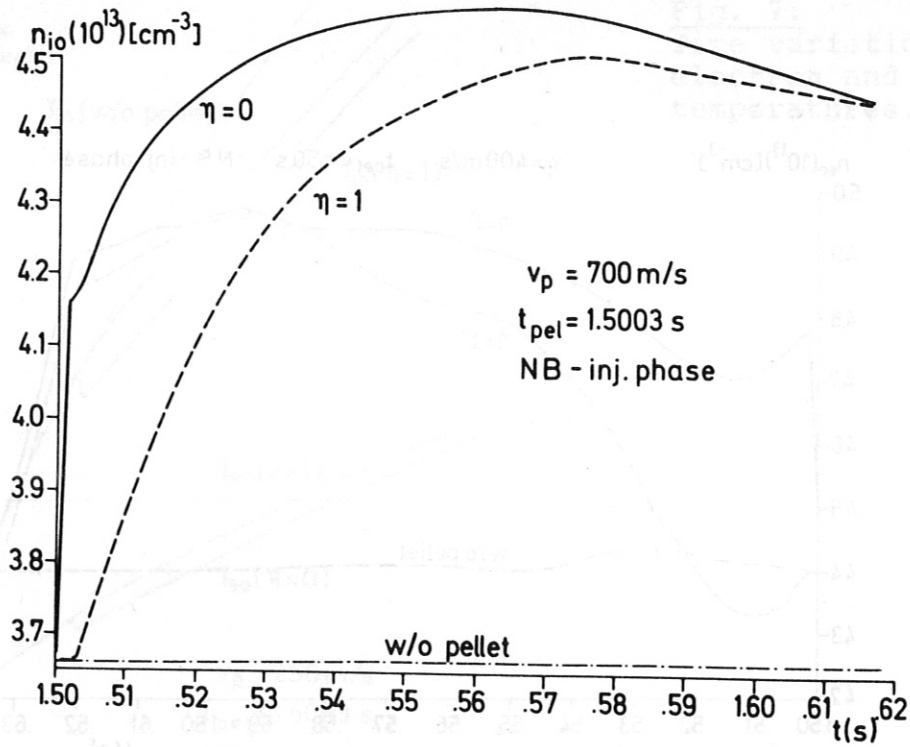

Fig. 11: Time variation of the central ion density.

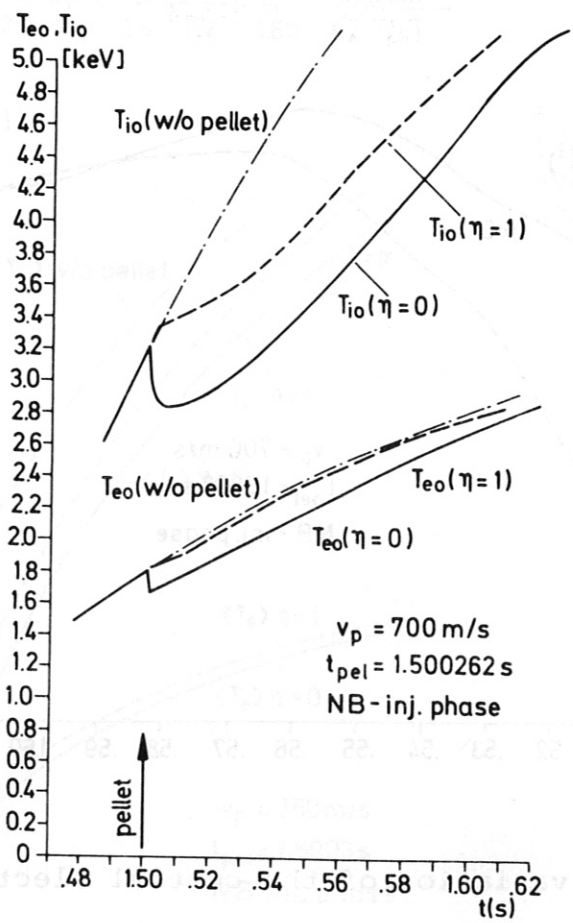

Fig. 12: Time variation of the central electron and ion temperatures.

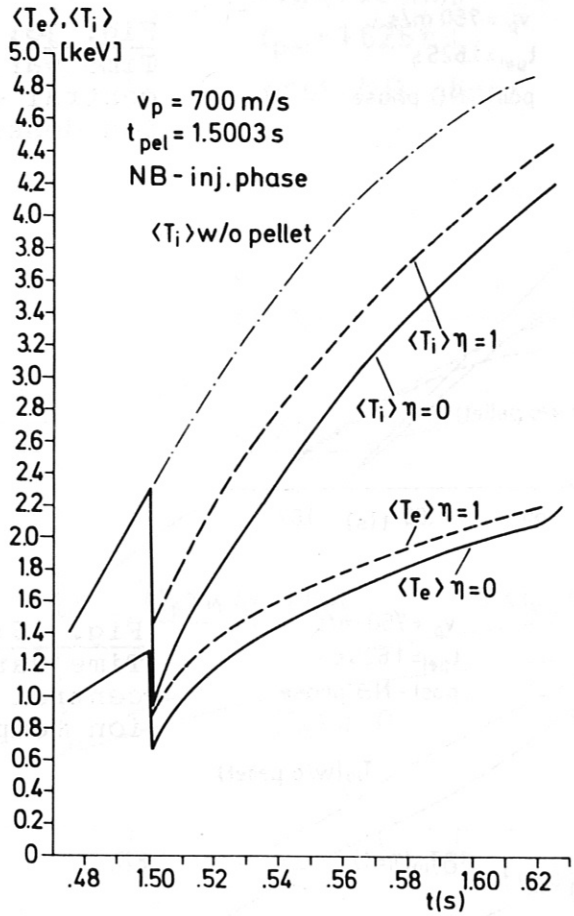

Fig. 13:
Time variation of the mean electron and ion temperatures.

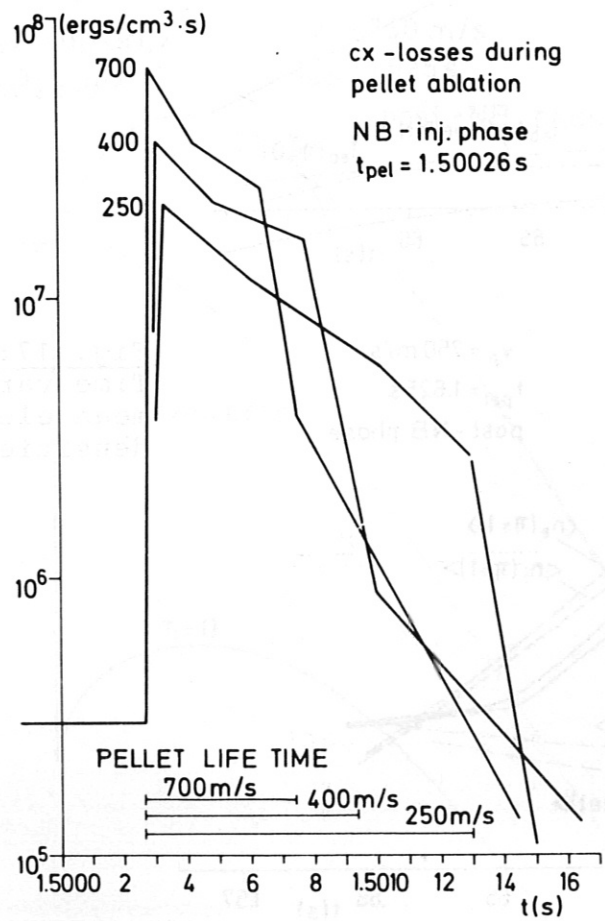

Fig. 14:
Energy losses caused by charge exchange collisions for different pellet velocities (NB-phase).

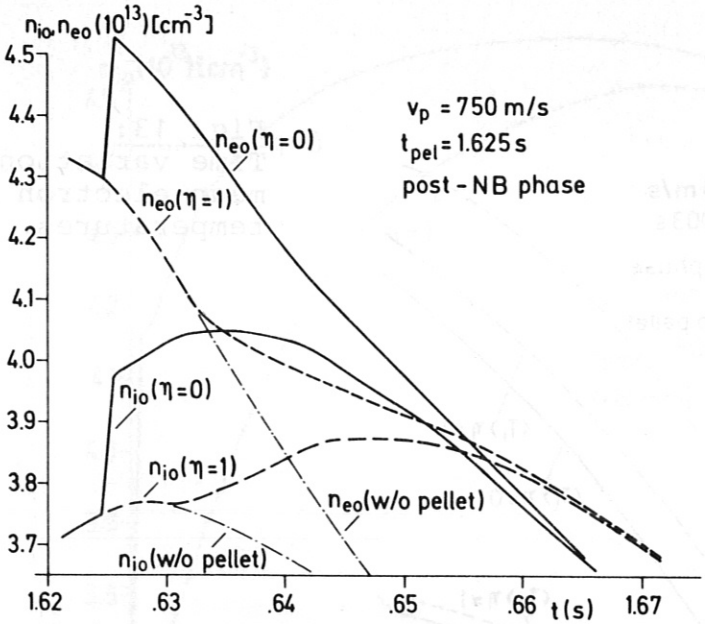

Fig. 15:
Time variation of the central electron and ion densities.

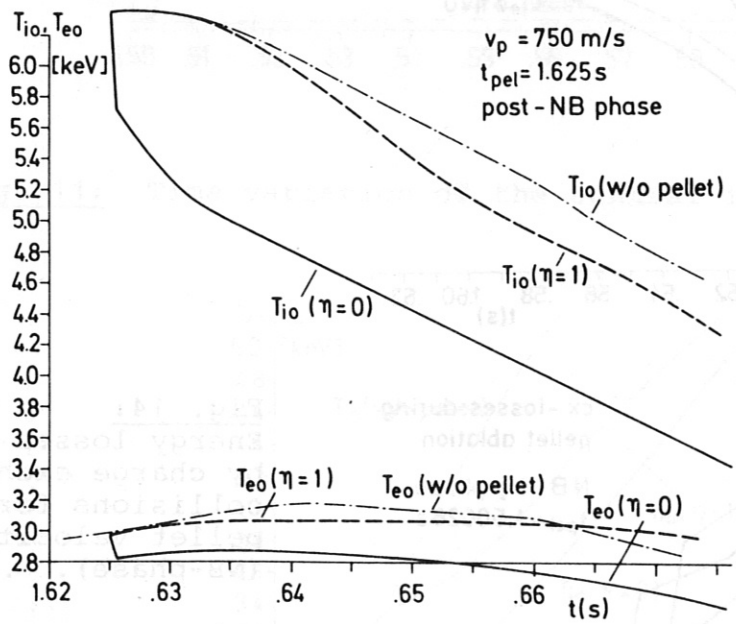

Fig. 16:
Time variation of the central electron and ion temperatures.

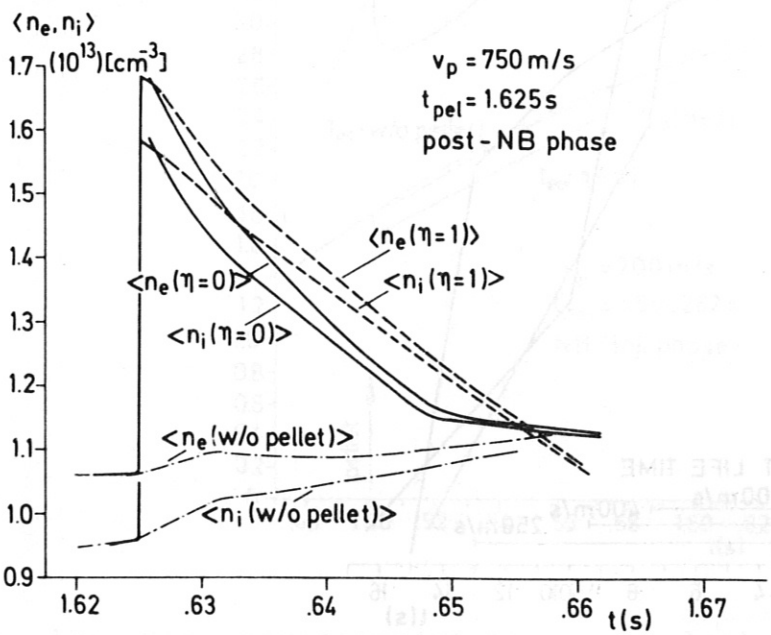

Fig. 17:
Time variation of the mean electron and ion densities.

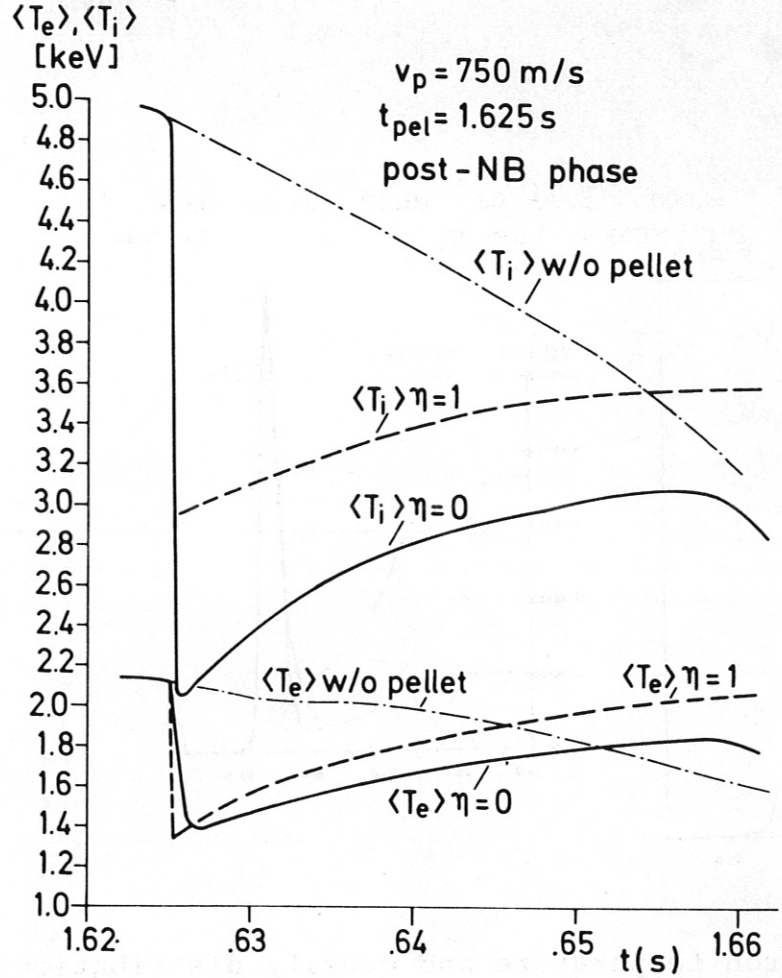

Fig. 18:
Time variation of the mean electron and ion temperatures.

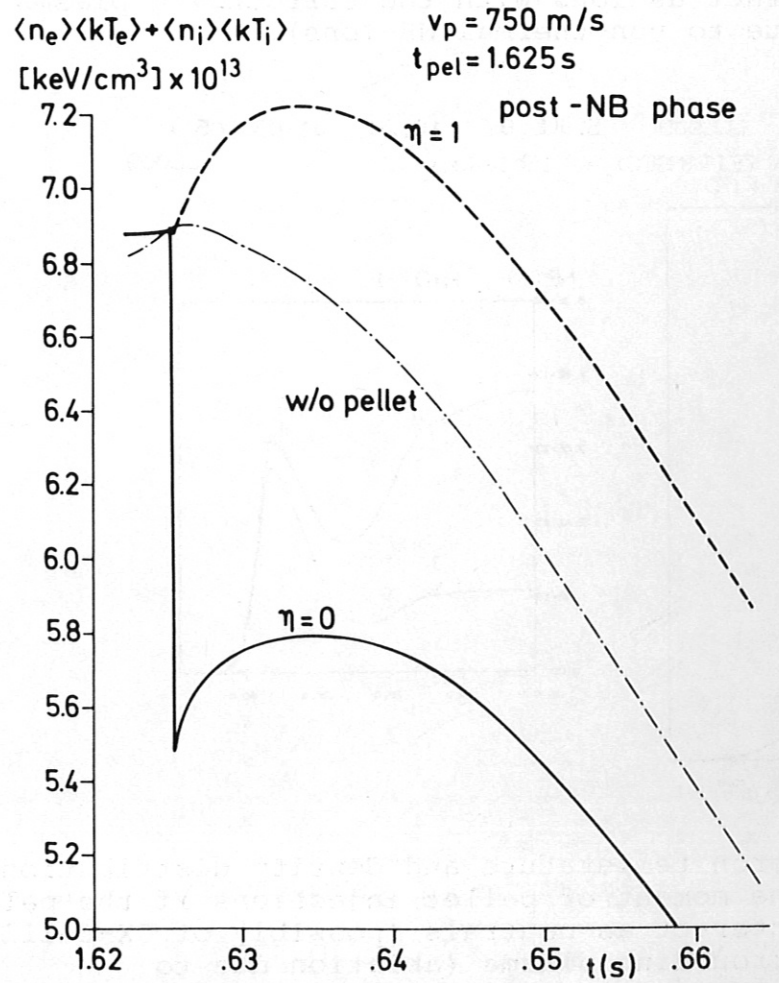

Fig. 19:
Time variation of the specific energy of the plasma during pellet injection.

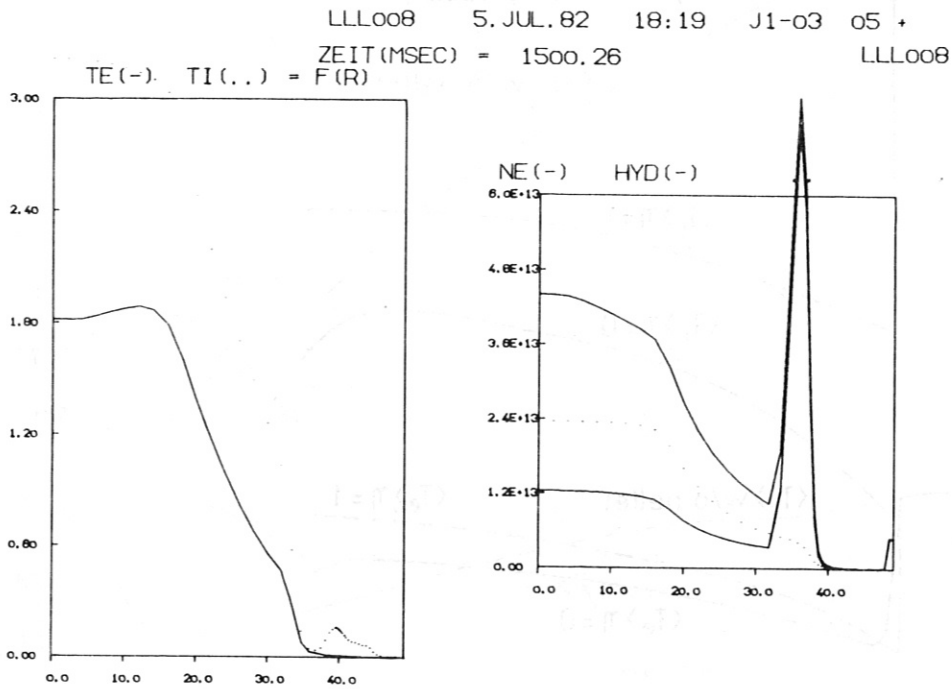

Fig. 20: Radial electron temperature and density distributions following the moment of pellet injection if the pellet particles interact as ions with the surrounding plasma (ablation due to non-thermal NB-ions).

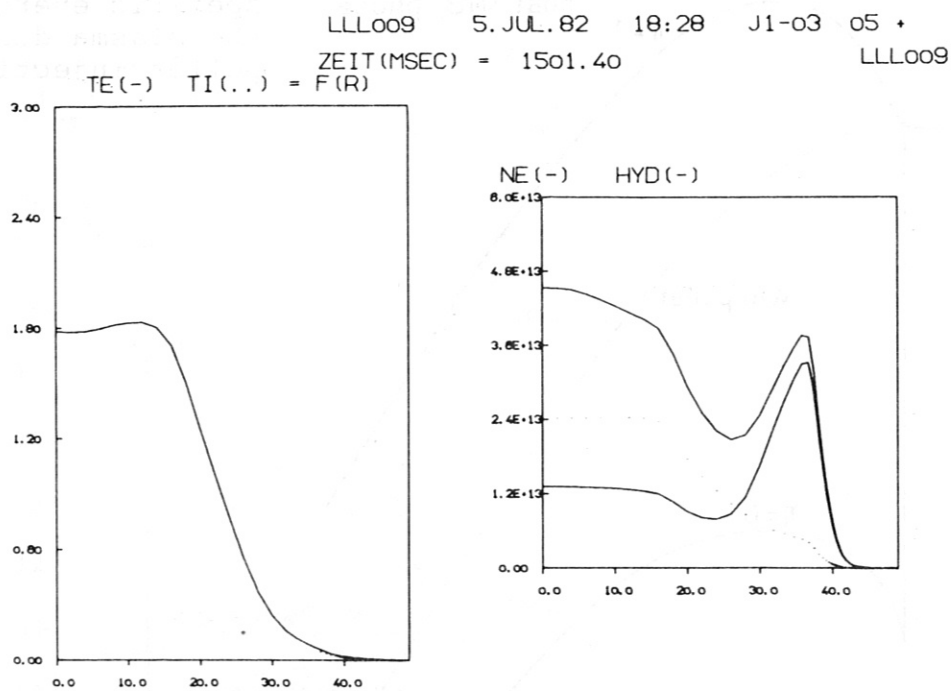

Fig. 21: Radial electron temperature and density distributions following the moment of pellet injections if the pellet particles interact as neutrals (possibly of CX-collisions) with the surrounding plasma (ablation due to non-thermal NB ions).